

Montagna, Mattia; Lux, Thomas

**Working Paper**

## Contagion Risk in the Interbank Market: A Probabilistic Approach to Cope with Incomplete Structural Information

FinMaP-Working Paper, No. 8

**Provided in Cooperation with:**

Collaborative EU Project FinMaP - Financial Distortions and Macroeconomic Performance, Kiel University et al.

*Suggested Citation:* Montagna, Mattia; Lux, Thomas (2014) : Contagion Risk in the Interbank Market: A Probabilistic Approach to Cope with Incomplete Structural Information, FinMaP-Working Paper, No. 8, Kiel University, FinMaP - Financial Distortions and Macroeconomic Performance, Kiel

This Version is available at:

<https://hdl.handle.net/10419/102271>

**Standard-Nutzungsbedingungen:**

Die Dokumente auf EconStor dürfen zu eigenen wissenschaftlichen Zwecken und zum Privatgebrauch gespeichert und kopiert werden.

Sie dürfen die Dokumente nicht für öffentliche oder kommerzielle Zwecke vervielfältigen, öffentlich ausstellen, öffentlich zugänglich machen, vertreiben oder anderweitig nutzen.

Sofern die Verfasser die Dokumente unter Open-Content-Lizenzen (insbesondere CC-Lizenzen) zur Verfügung gestellt haben sollten, gelten abweichend von diesen Nutzungsbedingungen die in der dort genannten Lizenz gewährten Nutzungsrechte.

**Terms of use:**

*Documents in EconStor may be saved and copied for your personal and scholarly purposes.*

*You are not to copy documents for public or commercial purposes, to exhibit the documents publicly, to make them publicly available on the internet, or to distribute or otherwise use the documents in public.*

*If the documents have been made available under an Open Content Licence (especially Creative Commons Licences), you may exercise further usage rights as specified in the indicated licence.*

# FinMaP-Working Paper No.8



This project has received funding from the European Union's Seventh Framework Programme for research, technological development and demonstration under grant agreement no. 612955



FINMAP –

**FINANCIAL DISTORTIONS AND MACROECONOMIC  
PERFORMANCE: EXPECTATIONS, CONSTRAINTS AND  
INTERACTION OF AGENTS**

DATE

TITLE

Contagion Risk in the Interbank Market: A  
Probabilistic Approach to Cope with  
Incomplete Structural Information

by: Mattia Montagna and Thomas Lux

## ABSTRACT

Banks have become increasingly interconnected via interbank credit and other forms of liabilities. As a consequence of the increased interconnectedness, the failure of one node in the interbank network might constitute a threat to the survival of large parts of the entire system. How important this effect of “too-big-too-fail” and “too-interconnected-too-fail” is, depends on the exact topology of the network on which the supervisory authorities have typically very incomplete knowledge. We propose a probabilistic model to combine some important known quantities (like the size of the banks) with a realistic stochastic representation of the remaining structural elements. Our approach allows us to evaluate relevant measures for the contagion after default of one unit (i.e. number of expected subsequent defaults, or their probabilities). For some quantities we are able to derive closed form solutions, others can be obtained via computational mean-field approximations.

*JEL-Classification: D85, G21, D83*

*Keywords: contagion, interbank market, network models*

## AUTHORS

1. **Mattia Montagna**

Kiel University  
Department of Economics  
Olshausenstr. 40-60  
24098 Kiel

Institute for the World Economy  
Kiellinie 66  
24105 Kiel

Email: [mattia.montagna@ifw-kiel.de](mailto:mattia.montagna@ifw-kiel.de)

2. **Thomas Lux**

Kiel University  
Department of Economics  
Olshausenstr. 40-60  
24098 Kiel

Bank of Spain  
Chair in Computational Economics  
University Jaume I  
Castellón, Spain

Email: [lux@bwl.uni-kiel.de](mailto:lux@bwl.uni-kiel.de)

# Contagion Risk in the Interbank Market: A Probabilistic Approach to Cope with Incomplete Structural Information\*

MATTIA MONTAGNA<sup>†</sup>, THOMAS LUX<sup>‡</sup>

## Abstract

Banks have become increasingly interconnected via interbank credit and other forms of liabilities. As a consequence of the increased interconnectedness, the failure of one node in the interbank network might constitute a threat to the survival of large parts of the entire system. How important this effect of “too-big-too-fail” and “too-interconnected-too-fail” is, depends on the exact topology of the network on which the supervisory authorities have typically very incomplete knowledge. We propose a probabilistic model to combine some important known quantities (like the size of the banks) with a realistic stochastic representation of the remaining structural elements. Our approach allows us to evaluate relevant measures for the contagion after default of one unit (i.e. number of expected subsequent defaults, or their probabilities). For some quantities we are able to derive closed form solutions, others can be obtained via computational mean-field approximations.

**JEL Classification:** D85, G21, D83

**Keywords:** contagion, interbank market, network models

## 1 Introduction

Systemic risk refers to the likelihood of a large portion of the financial system - potentially, the entire system - to jointly fail after an idiosyncratic shock, leading to a major disruption of capital allocation and risk transformation throughout the economic system. The consequences of systemic

---

\*The research reported in this paper is part of a research initiative launched by the Leibniz Community. It has been completed to a large part during a visit of the first author at the research group of the Banco de España at University Jaume I, Castellon. Helpful comments from the audience of various seminars and workshop presentations as well as stimulating discussions with Simone Alfarano are gratefully acknowledged. The research reported here has also benefited from funding from the European Union Seventh Framework Programme under grant agreement no. 612955.

<sup>†</sup>Department of Economics, University of Kiel and Kiel Institute for the World Economy, Germany, Email: mattia.montagna@ifw-kiel.de

<sup>‡</sup>Department of Economics, University of Kiel and Banco de España Chair in Computational Economics, University Jaume I, Castellón, Spain, Email: lux@bwl.uni-kiel.de.

events on the real economy have been dramatically revealed during the last financial crisis, directing the attention of academics and politicians towards new methodologies to study complex financial systems and the sources for systemic risk.

The probability of a large portion of the financial system to fail is governed by several direct and indirect connections among the individual financial institutions (hereafter, banks). Examples of direct connections are credit lines, interbank lending and derivative contracts. Indirect connections consist of spillover effects that one distressed institution can induce on any other, examples being fire sales and liquidity spirals (Brunnermeier (2009)). A link between two financial institutions always involves the transfer of a certain amount of risk between the banks' balance sheets. Because of the very nature of the financial system, the idiosyncratic risk of each institution is shared among its direct and indirect counterparties, which transfer some of the risk to their own counterparties, and so on. The result is a system in which the materialization of the risk in one bank can induce losses to spread among a large number of financial institutions, although they might not be directly connected with the bank in distress themselves.

In reality neither the banks themselves nor any other party might be able to exactly quantify the magnitude of risk that could be transmitted via the interbank network. This uncertainty could be completely removed if one had all the necessary information regarding interbank claims. However, this is often not possible, for various reasons. First, banks are not forced by law to report all of their connections to other banks<sup>1</sup>. Second, some components of the interbank network are evolving extremely fast, resulting in a practical impossibility to keep track of all prevailing interbank links<sup>2</sup>. Third, most of the transactions are still conducted in over-the-counter trades. In all such cases, a probabilistic representation reflecting this uncertainty could be very helpful to assess contagion risk.

The aim of this paper is to develop a probabilistic framework for the estimation of the probability of systemic events in a banking network of which only some key statistics and statistical regularities are known. Our work continues the recent line of research on the determinants and the modeling of systemic risk in stylized models of the topology of the interbank financial market. The pioneering work of Allen and Gale (2000) has first demonstrated the relevance of the structure of interbank linkages for the stability of the financial system in analytically solvable models with a few banks only. Subsequently, more general network approaches have been developed. Nier *et al.* (2007), have studied a random network structure for interbank liabilities. They demonstrate how the resilience of the whole system to id-

---

<sup>1</sup> And also if it were the case, this information would be available to regulators, but not to the single institutions, for which the problem would therefore persist.

<sup>2</sup> Examples are the overnight interbank network and the derivative network.

iosyncratic shocks is affected by the topological features of the system, such as the connectivity of the nodes. Alternative network structures have been studied by Iori (2008), Bluhm *et al.* (2013) and Georg (2013), among others. May and Arinaminphaty (2009) provide an analytical formulation of the results of Nier *et al.* using a mean-field approach, offering more general insights into the connections between complexity and stability. Another related analytical approach is Gai and Kapadia (2010) who use a stochastic framework based on the generating function methodology to the analysis of network structures as presented, e.g., in Newman (2013). Glasserman and Young (2014) derive theoretical bounds for the magnitude of contagion under different assumptions on the network structure and the heterogeneity of banks. The basic contribution of our approach to this nascent analytical literature is that we will focus on capturing certain stylized facts of the interbank market that are not captured yet in previous approaches. Our work is most closely related to May and Arinaminphaty (2009), but we relax two of the assumptions that are crucial in the derivation of their analytical solution, homogeneity in bank sizes and the Erdős-Rényi topology for the interbank network. We expand this line of research by providing a analytical and semi-analytical solutions for more general cases, where both the interbank network topology and the bank size distribution can take any form.

In order to apply our framework, we develop an algorithm aimed at generating financial systems capturing certain empirical “stylized facts” of interbank markets<sup>3</sup>. One pervasive finding in empirical data is disassortativity of link formation via interbank credit. In network theory, if high-degree vertices have a tendency to attach to low-degree ones, the resulting graph is said to display *disassortative mixing* or *disassortative behavior*. A simple way to identify such a structure consists in studying the distribution of the average degree of the neighbours of the vertices belonging to the network. In the case of disassortative mixing, this distribution should be a decreasing function of the degree of the nodes. Disassortative mixing has indeed been found to be a typical feature of many real networks, examples including the internet, the World Wide Web, protein interactions and neural networks (Caldarelli, 2007). Interestingly, essentially all interbank markets investigated so far seem to be characterized by disassortative behavior, as documented by Boss *et al.* (2004) for the Austrian interbank market, Soramäki *et al.* (2006) for the US Fedwire network, Iori *et al.* (2008) for the Italian interbank market, and Imakubu and Soejima (2006) for the Japanese interbank market. Therefore, it seems important to include this well-established stylized fact in the study of artificial financial networks, since this particular

---

<sup>3</sup> As in the case by Nier *et al.* (2007) and May and Arinaminphaty (2005), our networks are static since the single nodes are not allowed to change their behavior during the spread of the shock, but just absorb the propagation of losses.

structure could affect the ability of a system to absorb shocks.

Another feature that is often present in real networks is a characteristic power law distribution of the degrees (the number of connections across the units constituting the network). A power-law distributions of degrees also is the feature characterizing so-called *scale-free networks*. Scale-free networks are characterized also by the presence of hubs, namely nodes with a degree that is much higher than the mean degree of the other nodes. Therefore, in a scale-free network, there is a high probability that many transactions take place through one of the high-degree nodes of the network. The presence of such hubs makes a system in general more prone to a break-down in case of targeted attacks. This feature is the downside of their high connectivity that might contribute to an efficient channeling of flows providing short paths between any two nodes belonging to the system. Again, in real interbank money markets scale-free degree distributions have been frequently reported. Examples are Inaoka *et al.* (2004) and Imakubu and Soejima (2006) for the Japanese interbank market, and Boss *et al.* (2004) for the Austrian interbank market, while there exist divergent results for the Italian interbank market (Iori *et al.*, (2008), Fricke *et al.* (2012)).

We also believe that it is important to consider a realistic size distribution when studying the interbank network. As with firms size distributions in general (Luttmer (2007)), the distribution of the (balance sheet) sizes of banks is skewed to the right and at least close to a fat-tailed power-law distribution. As reported by Ennis (2001) and Janicki and Prescott (2006) for U.S. banks, the banking system is characterized by a large number of small banks and a few large banks, and the size distribution seems to be close to lognormal with a Pareto-distributed tail. A study on the evolution of the banking system in a European country can be found in Benito (2008), where the presence of few big hubs in the Spanish banking system is highlighted, and, again, the distribution is found to be highly skewed, and has become more skewed during the last decades. Glasserman and Young (2014) show how theoretical bounds on network effects depend on the heterogeneity of bank sizes and the distribution of links with both kinds of heterogeneity being crucial determinants for the extent of contagion effects.

We take the above three stylized facts into account in the design of our artificial banking system. In particular, we construct a Monte Carlo framework for an interbank market characterized by the above empirical features via what is called a *fitness algorithm* (De Masi *et al.*, 2006). With a particular choice of such a function as a generating mechanism for our network, we can make sure that our artificial banking sector displays a power law degree distribution together with disassortative link formation. As an immediate consequence, in an interbank market characterized by a power law in the size distribution, the default of a single small or medium-sized bank will mostly not affect the stability of the entire system: as one might expect, their losses are easily absorbed by their mostly large lenders, and typically

no domino effect occurs. The situation changes when the initially defaulting bank is one of the hubs of the system. In this case the propagation of the shock proceeds like the propagation of a circular wavefront in the water: starting from an initial node, the shock will hit at the same time all nodes that are directly linked to the source. Moreover, each time a new node is hit by the wave, it also will become a source of shock propagation itself, expanding the range of nodes that will potentially be affected by the shock. Those are the kind of network effects we are interested in.

Note that the results reported so far in the literature using network approaches in order to study domino effects in interbank markets have mostly used either random network models or networks constructed from aggregate data via a maximum entropy principle (cf. Upper, 2011, for an overview). Both approaches are very likely to underestimate the extent of a contagious spread of a disturbance due to the very homogeneous level of activity and connectivity in such artificial networks (as demonstrated, for example, by Montagna and Lux, 2013). In contrast, the above stylized facts show strong heterogeneity for the levels of activity (size of the balance sheets, as well as the extent of connectivity, namely the degree distribution). In addition, the pronounced negative assortativity is also not covered by random networks or those constructed from entropy principles. We might, therefore, expect a higher risk of contagion effects in models that share the above stylized facts.

The paper is organized as follows: Section 2 introduces the basic ideas of our probabilistic framework to measure systemic risk. Section 3 shows the algorithm we will use to generate interbank markets, demonstrating its ability to reproduce the above stylized facts. Section 4 applies the general probabilistic approach to this framework. Section 5 provides simple examples of contagion processes, and explains how the framework can be used to measure the systemic importance of single institutions. Section 6 uses more realistic shocks to perturb the banking system, by introducing correlation between banks' assets. Section 7 concludes.

## 2 The probabilistic framework

To assess financial stability we need a framework capable to measure the likelihood of systemic events. As our starting point, we consider the joint distribution of the equity levels of all the banks in the system. We denote by:

$$\Phi(\eta_1, \eta_2, \dots, \eta_N) \tag{1}$$

the joint distribution of equity levels  $\eta_i$ , for a financial system composed of  $N$  banks  $i = 1, 2, \dots, N$ <sup>4</sup>.

---

<sup>4</sup> We will specify later a complete structure for the banks balance sheets. In the present section, the framework we introduce is independent of the shape and composition of assets and liabilities, as well as of the possible direct and indirect mechanisms that propagate



In assessing the financial stability of the system, we are interested in studying how the distribution  $\Phi$  evolves after a shock hits the system. The uncertainty on the level of equity of banks can be due to two reasons. First, there could be incomplete information regarding the structure of the financial system. In this case, a pre-determined shock will generate several scenarios for the evolution over time given the initial configuration of the system: assigning a probabilistic weight to each of them will result in a joint distribution for the equity levels. Second, the shock itself could be described as a draw from of a stochastic variable. Even if the structure of the financial system were completely known, one would need to investigate the resulting scenarios through a probabilistic perspective. The known data on current balance sheet sizes would then be used as initial condition, and ignorance on the composition of the balance sheet and the existing interbank links would constitute the source of uncertainty.

Let us indicate with  $S$  a shock hitting the system at time  $t = 0$ . This shock can assume several forms: it can be a deterministic shock to a single institution, e.g. the default of a certain amount of its loan portfolio, it can be a probabilistic shock to a set of banks, specifying a correlation structure among the single shock components which reflect the correlation among their investments. Independently from its form, the shock will generally change the initial configuration of banks' equity levels, and we indicate with:

$$\Phi(\vec{\eta}|S) = \Phi(\eta_1, \eta_2, \dots, \eta_N; S) \quad (2)$$

the distribution of the equity levels conditional on the shock  $S$ . In all that follows, we will refer to eq. (2) as the  $\Phi$ -function of the financial system conditional on the shock  $S$ . From the joint distribution 2 it will be possible to quantify the probability of systemic events after an exogenous shock  $S$ , taking into account the incomplete structural information on the financial system. We explore in the following several examples for the use of our framework.

We start by considering the case where the shock  $S$  consists in wiping out a certain percentage of assets  $\lambda$  from bank  $i_0$ ; the shock  $S$  can be therefore represented by the  $N$ -dimensional vector  $\vec{s} = (0, 0, \dots, \lambda_{i_0}, \dots, 0) = s_{i_0}$ . The function  $\Phi(\vec{\eta}|\vec{s})$  includes all the information regarding the losses suffered by the other banks after the default of bank  $i_0$ , and can therefore be used to develop measures for its systemic importance. The expected number of

---

the shock from one institution to the other.

defaults  $\langle \tilde{N} | s_{i_0} \rangle$  is computed as:

$$\begin{aligned} \langle \tilde{N} | s_{i_0} \rangle &= \langle \sum_{i=1}^N (1 - \theta(\eta_i)) | \vec{s} \rangle = \sum_{i=1}^N \langle (1 - \theta(\eta_i)) | \vec{s} \rangle = \\ &= \sum_{i=1}^N \int_{-\infty}^{+\infty} d\eta_1 \int_{-\infty}^{+\infty} d\eta_2 \dots \int_{-\infty}^0 d\eta_i \dots \int_{-\infty}^{+\infty} d\eta_N \Phi(\vec{\eta} | \vec{s}) \end{aligned} \quad (3)$$

where we indicated with  $\theta(\cdot)$  the classical Heaviside function. The mean number of defaults computed in eq. (3) is a first indicator of the systemic importance of a financial institution. In fact, it quantifies the spillover effects coming from the default of bank  $i_0$ . Nevertheless, the above expression can underestimate systemic importance since it ignores the events populating the tails of the distribution  $\Phi$ , as well as a possible correlation structure among banks' balance sheets. To overcome this problem, another choice could be to compute the probability to observe a certain number  $\tilde{N}$  of defaults given the defaults of bank  $i_0$ , that is  $Pr[\tilde{N} | s_{i_0}]$ , which can be computed as:

$$Pr[\tilde{N} | s_{i_0}] = c \cdot \sum_{\Pi} \int_{-\infty}^0 d\eta_1 \dots \int_{-\infty}^0 d\eta_{\tilde{N}} \dots \int_0^{\infty} d\eta_N \Phi(\vec{\eta} | s_{i_0}) \quad (4)$$

where  $\Pi$  represents all possible permutations of the indexes  $i$ ,  $c$  being a normalization factor:

$$c = \left( \frac{\tilde{N}!}{N!(N - \tilde{N})!} \right)^{-1} \quad (5)$$

The quantity expressed in eq. (4) can be seen as the systemic value at risk conditional on the initial shock  $S$ .

The shock  $S$  can also be described by a set of stochastic variables. Let's consider therefore a vector of random variables  $\vec{\Lambda} = (\Lambda_1, \Lambda_2, \dots, \Lambda_N)$ . The distribution of the  $i$ -th component  $\Lambda_i$  could, for instance, be extracted from the profit-loss distribution of banks. Moreover, a correlation structure among the  $N$  variables can be specified and it will play a fundamental role in assessing the probability of joint failures in the system, i.e. systemic events. Given the distribution  $\Phi(\vec{\eta} | \vec{\Lambda})$ , another interesting quantity one may want to compute is the extreme  $q$ -quantile of the distribution of the number of defaults following the stochastic shock  $\vec{\Lambda}$ . If we call  $\phi(\tilde{N} | \vec{\Lambda})$  the distribution of the number of defaults conditional on the shock  $\vec{\Lambda}$ , that is:

$$\phi(\tilde{N} | \vec{\Lambda}) = Pr[\tilde{N} | \vec{\Lambda}] \quad (6)$$

the extreme  $q$ -quantile of this distribution,  $N_q$ , defined as:

$$\int_0^{N_q} dx \phi(x | \vec{\Lambda}) = (1 - q) \quad (7)$$

measures the fatness of the tail of the joint distribution where systemic events are happening.

The above set of measures to detect systemic importance of institutions and to assess systemic risk can be further enriched depending on the particular scenarios one wants to analyze, and on the available data. In the following, we concentrate on one particular mechanism of contagion among financial institutions, which is direct interbank exposure through bilateral loans. For this mechanism of contagion, we are able to analytically compute some of the above quantities, while others can be easily computed through numerical algorithms. We highlight again that, due to the generality of the framework we introduced, including other forms of interbank contracts is straightforward, at least from a computational point of view. The goal of the paper is to provide a framework based on statistical tools and basic assumptions on the contagion mechanism to capture "probabilities" of contagious events based upon empirically plausible distributional assumptions for the observed structural features of the financial network. In order to test our approach on a simulated interbank market, we introduce in the next section an algorithm which (i) is able to reproduce the most common features of real interbank lending networks; (ii) allows to include eventual uncertainty one has on the structure of the banking system; and (iii) is easy to implement and calibrate. Then, we show how to compute the quantities expressed above, and how they can play a role in assessing systemic risk.

### 3 The structure of the banking network

We consider an interbank market (IbM) composed of  $N$  financial entities linked together by their claims on each other. Each bank in the IbM will be represented as a node in the network, and the information of the loans among banks will constitute the edges of the network. These edges are directed and weighted, the weight of the link starting from node  $i$  and pointing to node  $j$  being the total amount of money that bank  $i$  lends to bank  $j$ . The structure of our model will be set up in a way to represent certain documented empirical features. Following Nier *et al* (2007), we use the scheme in Fig. 1 to represent the balance sheets of banks. The assets  $A_i$  of each bank ( $i = 1, 2, \dots, N$ ) are partitioned into interbank loans  $l_i$  and external assets  $e_i$ :

$$A_i = l_i + e_i \quad (8)$$

The liabilities  $I_i$  of each bank are partitioned into interbank borrowing  $b_i$  and customers' deposits  $d_i$ :

$$I_i = b_i + d_i \quad (9)$$

Solvency requires that the difference between a bank's assets and its liabilities be positive, that is:

$$\eta_i \equiv (l_i + e_i) - (d_i + b_i) \geq 0 \quad (10)$$

where we denote bank  $i$ 's net worth by  $\eta_i$ .

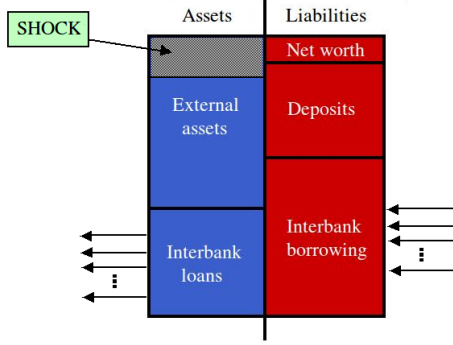


**Fig. 1:** The balance sheet structure of each bank  $i$  belonging to the IbM.

If relationship (10) is not fulfilled, bank  $i$  becomes insolvent. Note that we could instead impose a minimal capital requirement and intercept the bank's operations if its capital falls below a certain threshold. For most purposes this would leave our results qualitatively unchanged as it would just lead to a linear rescaling of the balance sheet. However, our analytical representation of an insolvency cascade is facilitated by a zero threshold for the default of a financial institution.

Following Nier *et al.* (2007), we impose the following relations, that hold for all banks belonging to the IbM:

$$e_i = \theta A_i \quad (11)$$

$$l_i = (1 - \theta) A_i \quad (12)$$

$$\eta_i = \gamma A_i \quad (13)$$

i.e., external assets, interbank loans and net worth are determined (initially) as fixed functions of total assets. This enables us to characterize the evolution of the balance sheet of the banks using the common pair of parameters  $\theta$  and  $\gamma$ . Unlike Nier *et al.* (2007) who investigate a banking sector with banks of equal size of balance sheets and interbank liabilities, we, however, try to mimic some of the documented dimensions of heterogeneity in the banking sector via the distribution of banks' size and that of the links between banks.

The empirical properties of real interbank networks that we attempt to reproduce are the disassortative behavior and the power law in the degree and size distributions. To this end, we arrange the nodes on a scale free network according to the following algorithm, based on Montagna and Lux (2013):

1. we start with an assumption on the distribution of the size of the banks. Using  $A_i$  as parameter indicating the size of a bank, we assume that  $\rho(A_i) \propto A_i^{-\tau}$  (and  $A_i \in [a, b]$ ) so that the size distribution will follow a

power law over the interval between  $a$  and  $b$  determining the minimum and maximum size of a bank in our system. In the following we will use  $\tau = 2$ . We note that since this formalism defines the size distribution over a finite range, the numbers  $a$  and  $b$  defining the absolute range of bank sizes will also be of some relevance.

2. once we have drawn the  $N$ -element set  $\{A_i\}$  i.e. the distribution of the total assets of the banks, we compute the external assets  $e_i$ , the sum of interbank loans  $l_i$  and the net worth  $\eta_i$ , according to eqs. (11) - (13).
3. we now denote the size parameter  $A_i$  as the *peculiarity* of the node. We add interbank liabilities to the system taking into account the banks' peculiarity. In order to build up networks in this way, we use a *probability function*  $P(A_i, A_j)$ : this function provides the probability that a bank  $i$  (characterized by total external assets  $A_i$ ) lends money to bank  $j$  (characterized by total external assets  $A_j$ ). It has typically been found in empirical data of interbank credit relations that a pool of small and medium-sized banks mostly lend money to the largest banks of the system, which in turn redistribute liquidity to external financial markets or within the system itself (Iori *et al.* (2008), Cocco *et al.* (2009), Fricke and Lux (2012)). The choice of an appropriate probability function allows to reproduce those important empirical observations. In this paper, we will use the following alternative probability functions:

$$P_1(A_i, A_j) = d_1 \cdot \left(\frac{A_i}{A_{max}}\right)^\alpha \cdot \left(\frac{A_j}{A_{max}}\right)^\beta \quad (14)$$

$$P_2(A_i, A_j) = d_2 \cdot (A_i + A_j) \quad (15)$$

$$P_3(A_i, A_j) = d_3 \cdot H(A_i + A_j - z) \quad (16)$$

where  $A_{max}$  denotes the size of the balance sheet of the largest bank in the system,  $\alpha$ ,  $\beta$  and  $z$  are constants, and  $H(x)$  is the Heaviside step function.  $d_1$ ,  $d_2$  and  $d_3$  can be used to adjust the density of the networks. The next section will present the main topological properties of networks produced by functions (14), (15) and (16). With any of these probability functions, we can build an  $N \times N$  probability matrix  $P \in M_{N \times N}$ , with entries  $p_{ij} = P_s(A_i, A_j) \in [0, 1]$  determining the probability for the link between  $i$  and  $j$ , and  $s = 1, 2, 3$ ;

4. the next step consists in constructing the adjacency matrix  $A$  of the network, according to the rule:

$$a_{ij} = \begin{cases} 1, & \text{with probability } p_{ij} \\ 0, & \text{with probability } (1 - p_{ij}) \end{cases}$$

In this way we reproduce the systematic tendency of accumulation of links at larger entities. As we will show below, these functions also allow us to reproduce the disassortative nature of empirical banking networks<sup>5</sup>;

5. we also assume that the volume of loans reflect banks' *peculiarity*; it seems natural to assume that financial entities will have more intense links with banks with high peculiarity (balance sheet size). Including this notion in the probability functions we compute the load  $l_{ij}$  (the volume of credit) of the link between bank  $i$  and bank  $j$  as:

$$l_{ij} = \frac{l_i p_{ij}}{\sum_{j \in \Omega_i} p_{ij}} \quad (17)$$

where  $\Omega_i$  denotes the set of nodes for which  $a_{ij} = 1$ ;

6. in the last step, we compute the internal borrowing  $b_i$  as:

$$b_i = \sum_{j=1}^n l_{ji} \quad (18)$$

and the customers' deposits  $d_i$  as:

$$d_i = (e_i + l_i) - (\eta_i + b_i) \quad (19)$$

Deposits are, thus, the residual in the construction of the balance sheets of banks that is adjusted in a way to guarantee consistency. While this leads to a certain degree of heterogeneity of the role of deposits across banks, this is not necessarily an unrealistic feature of our system, as banks rely to a different degree on different sources of funding.

Let us also emphasize that in the algorithm there are two levels of randomness: the first appears in step 1, in the determination of the sizes of the nodes, while the second appears in step 4, in the realization of the probability matrix. Thus, for a fixed sequence of the sizes  $\{A_i\}$ , various realizations of the network are possible. Given current data availability for the financial sector, a most plausible implementation of our framework might consider the bank sizes as known data but the link structures as the unknown realization of the stochastic process specified above.

The probability functions reflect the micro behavior of banks when selecting their counterparties in the interbank market, and they assume a

---

<sup>5</sup> It is possible especially for symmetric probability functions, to encounter situations where  $a_{ij} = a_{ji} = 1$ . Since loops are not allowed in our model (they would mean that bank  $i$  and  $j$  are both borrower and lender of each others), we have to add a rule for the elimination of one of the edges. A possible choice is to randomly eliminate one of the two links  $i \rightarrow j$  or  $j \rightarrow i$ . However, other choices are possible as well, if the aim is to enforce the disassortative behavior of the networks.

crucial role in the determination of the characteristics of the financial system. One of the main features of these networks is the presence of power laws in the degree distributions of both *in*- and *out*-degree. In particular, one can show that using the probability functions (14), (15) and (16), one obtains, respectively the following approximate distributions for in-degree and out-degree,  $k_{in}$  and  $k_{out}$ , under the three different generating mechanisms<sup>6</sup>:

$$P_1(k_{in}) \propto k_{in}^{-\frac{1+\beta}{\beta}}, \quad P_1(k_{out}) \propto k_{out}^{-\frac{1+\alpha}{\alpha}} \quad (20)$$

$$P_2(k_{in}) \propto (c_1 k_{in} + c_2)^{-2}, \quad P_2(k_{out}) \propto (c_3 k_{out} + c_4)^{-2} \quad (21)$$

$$P_3(k_{in}) \propto k_{in}^{-2}, \quad P_3(k_{out}) \propto k_{out}^{-2} \quad (22)$$

In the same way, it is possible to see that the average degree of a neighbour is determined by:

$$\langle k_{nn} \rangle (A_i) = \frac{N}{k(A_i)} \cdot \int_a^b p(A_i, t) k(t) \rho(t) dt \quad (23)$$

where  $k(A_i)$  is the mean *total degree* of node  $i$ , as a function of its own fitness parameter.

The density of the network generated by the probability functions (20) to (22) is:

$$D^l = \frac{2 \sum_{i,j=1}^N p_{ij}^l}{N(N-1)} \propto d_l \quad (24)$$

where  $l = 1, 2, 3$ . The density of the networks can therefore be easily manipulated via the parameters  $d_l$ , keeping fixed the other topological features. In case of a constant probability function  $P(A_i, A_j) = d$ , networks produced are random with density equal to  $d$ .

As we can see, with all three kinds of probability functions, the results are scale-free networks (i.e., a power-law distribution of degrees). Since eq. (23) involves the mean total-degree of a node,  $k(A_i)$ , there is no closed-form solution for this expression for the three probability functions. The disassortative behavior can, however, be confirmed via numerical integration of eq.(23), cf Fig. 2. It is apparent from eqs. (20) to (22), that it will be possible to change the exact shape of the degree distributions as well as the degree of disassortative behavior by modifying the parameters of the probability functions, and the distribution of the fitness parameters. Fig. 2 shows the simulated degree distributions and the average neighbour degree for functions (14), (15) and (16), for parameters  $\alpha = 0.2$ ,  $\beta = 1.2$  and

<sup>6</sup> Cf. Caldarelli (2007). The main steps in deriving in-degree and out-degrees distributions are also detailed in the Appendix.

$z = 0.5 \cdot A_{max}$ ; finally,  $d_1 = d_2 = d_3 = 1$ . With this choice of the parameters we get tail indexes in the in- degree distribution equal to, respectively,  $-1.83$ ,  $-2$  and  $-2$ , and  $-6$ ,  $-2$  and  $-2$  for the out-degree distributions. Moreover, a clear disassortative behavior is observed in all the three cases<sup>7</sup>.

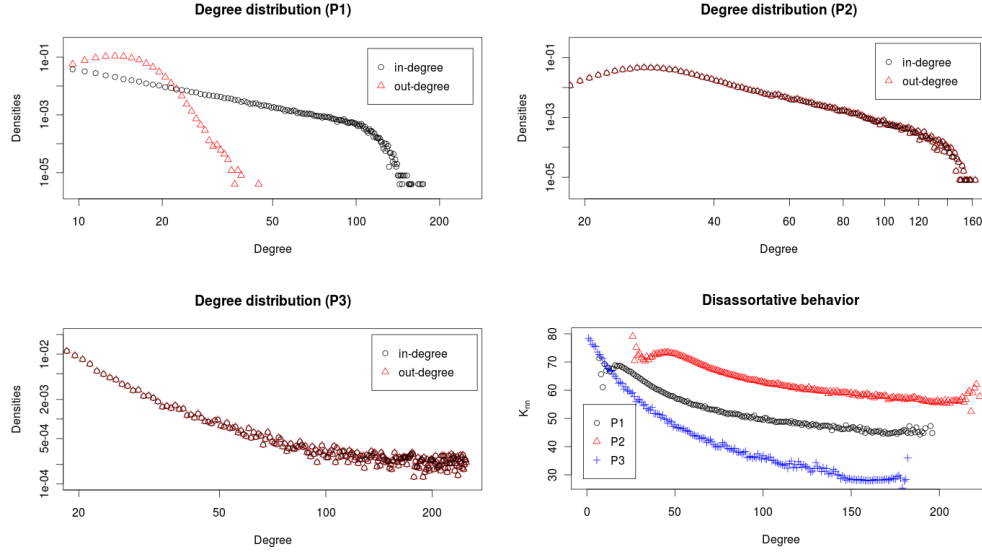


**Fig. 2:** The first three panels show the *in-* and *out-degree* distributions for the three probability functions (14), (15) and (16). The last panel shows the mean neighbour degree as a function of the *total degree* of the nodes. The curves in the last panel are decreasing with the degree itself, indicating that big nodes are connected to a multitude of small and medium-sized nodes, which themselves are connected with only a (relatively) small number of hubs.

## 4 Single Shocks and Network Risk

We now combine the probabilistic framework introduced in Sec. 2 and the algorithm introduced in Sec. 3 to assess how the financial stability of the banking system is affected by the main parameters of the model. The shock  $S$  in this section will consist in wiping out a percentage of the external assets of the largest bank in the system, so it can be written as  $\vec{s} = (0, 0, \dots, \lambda_{i_0}, \dots, 0) = s_{i_0}$ , where  $i_0$  is the largest bank. In this scenario, the only uncertainty is due to the missing information regarding the

<sup>7</sup> In order to reinforce the disassortative behavior, one could use a criterion for the elimination of the loops different from the one described in footnote 5. In particular, if both the edges  $i \rightarrow j$  and  $j \rightarrow i$  are present in the network, one could eliminate the one starting from the biggest node of the two: this mechanism would contribute to tuning the system even more towards the characteristics of real interbank network structures, where mostly small banks lend money to big banks, as described in the introduction.



structure of the banking system, represented by the probability functions introduced in Sec. 3. In particular, we will use function (14) to generate our interbank networks, and we will explore how the parameters  $\gamma$  and  $\theta$  affect the stability of the banking system.

When the largest bank in the system fails, the other banks can suffer losses in two ways. The first way is through direct contagion. In fact, the initial loss is first absorbed by the bank's net worth  $\eta_{i_0}$ , then by its interbank liabilities  $b_{i_0}$  and last its deposits  $d_{i_0}$ , as the ultimate *sink*. That is, we assume priority of (insured) customer deposits over bank deposits which, in turn, take priority over equity (net worth). If the bank's net worth is not large enough to absorb the initial shock, the bank defaults and the residual is transmitted to creditor banks through interbank liabilities. Creditor banks are assumed to receive an amount of the residual shock proportional to their exposure to the failed bank. Those banks will have to book losses in their equities<sup>8</sup>.

The second way banks can suffer losses is indirect contagion through network effects. In fact, in case the direct creditors of the initial failing bank are not able to absorb the losses, they will fail and transmit losses to their own creditors. The process continues until the losses are completely absorbed by the system or, alternatively, the whole system has failed.

It seems natural when studying the loss propagation process to formally introduce a discrete event index  $t$  describing the different phases of the propagation of the shock. We call that index the *round* of propagation. We start from a situation in which the system is in a stationary state with positive net worth of all banks, and at a certain point  $t = 0$  we subject one bank,  $i_0$ , to a shock by wiping out a fraction  $\lambda_{i_0}$  of its external assets<sup>9</sup>. At event time  $t = 0$  no other banks will incur any losses, but part of the assets of the initially shocked bank have been destroyed, and so we can write:

$$\Phi^{t=0}(\eta_1, \eta_2, \dots, \eta_n | s_{i_0}) = \delta\left(\eta_{i_0} - \left(\eta_{i_0}^0 \cdot \frac{\gamma - \lambda_{i_0}\theta}{\gamma}\right)\right) \cdot \prod_{i=1, i \neq i_0}^N \delta(\eta_i - \eta_i^0) \quad (25)$$

where  $\delta(x)$  is the Dirac delta, and  $\eta_i^0$  are the net worths of the banks before the shock starts propagating. If we apply now eq. (3) we obtain:

$$\bar{N}^{t=0} = \begin{cases} 1, & \text{if } \gamma \leq \lambda_{i_0}\theta \\ 0, & \text{otherwise} \end{cases} \quad (26)$$

<sup>8</sup> We disregard partial recovery of the defaulted loans as this will happen only much later during bankruptcy proceeding and would be of little relevance to the unfolding short-run dynamics.

<sup>9</sup> We note here that restricting ourselves to the case of a single shocked unit does not restrict the generality of our approach. In fact, simultaneous deterministic shocks to different banks at the same time can be represented as the convolution of multiple  $\Phi$ -functions.

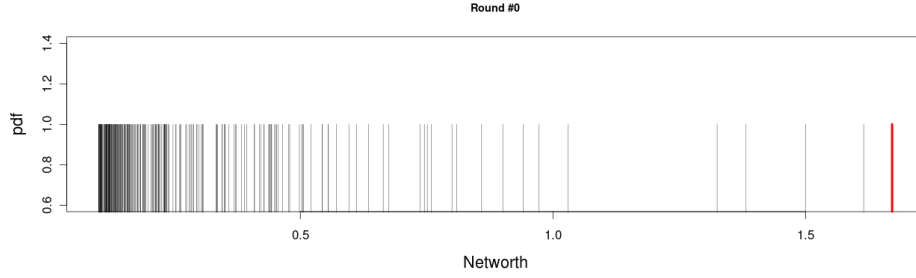


**Fig. 3:** The figure schematically shows the  $\Phi$ -function at round zero, i.e. eq. (25). At time  $t = 0$  all the banks have a well-defined non-stochastic net worth  $\eta_i$ , represented in the figure by a vertical line of length 1, i.e. the probability for each bank to have net worth  $\eta_i$  to be exactly 1. The red line represents the largest bank in the IbM. The distribution of banks size has been drawn from a power-law distribution with tail parameter equal to 2.

and so the perturbation can start propagating only if the shock is large enough<sup>10</sup>. Fig. 3 shows an illustration of the function  $\Phi^{t=0}$  and the initially shocked bank  $i_0$  (red line). Note that, initially, the net worth of each bank is known with certainty, i.e. all values have probability 1 (vertical axis).

We can now move on to the next round; at time  $t = 1$  the variables  $\eta_i$  are still independent (and hence uncorrelated), and it is possible to factorize the  $\Phi$ -function as in the previous case:

$$\Phi^{t=1}(\eta_1, \eta_2, \dots, \eta_n | s_{i_0}) = \delta \left( \eta_{i_0} - \left( \eta_{i_0}^0 \cdot \frac{\gamma - \lambda_{i_0} \theta}{\gamma} \right) \right) \cdot \prod_{i=1, i \neq i_0}^N \Phi_i^{t=1}(\eta_i | s_{i_0}) \quad (27)$$

where  $\Phi_i^{t=1}(\eta_i | s_{i_0})$  represents the marginal distribution of the net worth of bank  $i$  at time  $t = 1$ . In the probabilistic determination of eq. (27) the stochastic representation of our ignorance of the details of interbank credit connections comes in. We assume that these connections are well represented by the probability function  $P(A_i, A_j)$  introduced in Sec. 3 that replicates important stylized facts of empirical data. In the Appendix we show that  $\Phi_i^{t=1}(\eta_i | s_{i_0})$  consists of two parts: with probability  $p_{ii_0}$  bank  $i$  will be affected in the first round of aftereffects after the initial shock, while with probability  $1 - p_{ii_0}$ , it will still remain unaffected at this stage (it is sufficiently remote from bank  $i_0$ ). The first case, then, leads to a loss due to the defaults of bank  $i_0$  on some of its interbank loans. In the absence of exact knowledge this effect is stochastic (to the outside observer or to the supervisory authority). We show in the Appendix that the size of the loss can be approximated by a Normally distributed random variable. The

<sup>10</sup> If  $N_0 = 0$ , the first bank is able to absorb the shock and no contagion effects will be registered in the system.

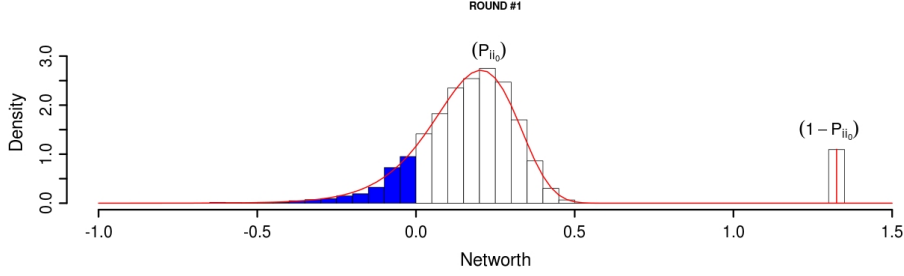


**Fig. 4:** The picture shows one of the marginal distribution functions described by eq. (28). Each of these distributions are composed by a Dirac delta centered on  $\eta_i^0$ , indicating that with probability  $(1 - p_{ii_0})$  bank  $i$  is not linked to bank  $i_0$  directly, and so its net worth will rest unchanged at time  $t = 1$ . The second component gives a contribution of the propagation of the initial shock if a link exists to bank  $i_0$  which happens with probability  $p_{ii_0}$ .

complete expression can be written as:

$$\Phi_i^{t=1}(\eta_i | s_{i_0}) = P_i^I \cdot \frac{b(\gamma, \theta)(a(\gamma, \theta) - \eta_i)^{-2}}{\sigma_1^i \sqrt{2\pi}} \exp \left\{ -\frac{1}{2} \left( \frac{\frac{b(\gamma, \theta)}{a(\gamma, \theta) - \eta_i} - m_1^i}{\sigma_1^i} \right)^2 \right\} + (1 - P_i^I) \delta(\eta_i - \eta_i^0) \quad (28)$$

where  $a(\gamma, \theta)$  and  $b(\gamma, \theta)$  are functions of the percentage of net worth and of the weight of the first term,  $P_i^I = p_{ii_0}$  is the probability for bank  $i$  to belong to the first shell of banks connected to  $i_0$ . Explicit equations for  $m_1^i$  and  $\sigma_1^i$  are presented in the Appendix, and both completely depend only on the topological features of the network and in the case of our probability functions (14) through (16) on the size of the balance sheet of the banks. We compute in the Appendix the mean value and the standard deviation for  $\Phi_i^{t=1}(\eta_i | s_{i_0})$ , and we show that its variance tends to zero when the entries of the probability matrix  $p_{ij}$  tend to 0 or 1, namely when the network becomes deterministic.

Fig. 4 shows an example of the marginal distributions  $\Phi_i^{t=1}(\eta_i | s_{i_0})$  for a single bank, and the blue area highlighted in the figure is the probability for that bank to fail. The marginal  $\Phi$ -function expressed in eq. (28) represents what can be defined as *first round effects*. In fact, banks subject to the potential losses in this first stage of the propagation are only the direct counterparties of the initial failing bank  $i_0$ . In the other stages of the shock propagation, instead, all the banks can potentially be subject to losses because of the network of interbank contracts, and we call them *higher round effects*. In general, a closed form solution for the  $\Phi$ -function describing higher round effects is hard to obtain. Although different types

of approximations are possible<sup>11</sup>, we prefer to generate random variables according to the joint distribution  $\Phi^t$  and compute numerically the integrals in eqs. (3), (4) and (7)<sup>12</sup>.

Figure 5 shows the temporal evolution from  $t = 1$  (round 1) to  $t = 2$  (round 2) of one of the marginal distributions  $\Phi_i^t(\eta_i | s_{i_0})$ . We immediately note from the graph that also the contribution linked to  $(1 - p_{ii_0})$  spreads out, due to possible connections of second order (i.e. credit expanded to the creditor banks of the initially defaulting one). This fact actually reflects the topology of the networks generated by probability function (14): the small diameter of these scale-free networks imposes that in two steps a node can mostly reach every other nodes, if the initially shocked bank is one of the biggest of the system. If we again consider the marginal distributions, we can split them up into three components, so that for round 2 we can formally write:

$$\Phi_i^{t=2}(\eta_i | s_{i_0}) = P_i^I \cdot \Phi_i^{t=2,I}(\eta_i | s_{i_0}) + P_i^{II} \cdot \Phi_i^{t=2,II}(\eta_i | s_{i_0}) + (1 - P_i^I - P_i^{II}) \cdot \delta(\eta_i - \eta_i^0) \quad (29)$$

where  $P_i^I$  is the probability for bank  $i$  to belong to the first shell with respect to the initially defaulting bank  $i_0$ , that is  $P_i^I = p_{ii_0}$ , and in general  $P_i^l$  is the probability for bank  $i$  to belong to the  $l$ th shell,  $l = I, II, III, \dots$ , with respect to bank  $i_0$ <sup>13</sup>. The contribution linked to  $(1 - P_i^I - P_i^{II})$  is a Dirac delta since in two rounds there is no way for the shock to hit banks belonging to the 3rd (or higher) shell. In the pink distribution of Fig. 5, representing a possible outcome of eq. (29) this contribution vanishes simply because with the underlying parameters  $P_i^I + P_i^{II} \simeq 1$ . In general, higher-order defaults can occur over many rounds.

Note that in the limit  $t \rightarrow \infty$ <sup>14</sup> the system will converge in probability to a steady state, defined by the  $\Phi$ -function  $\Phi^\infty(\eta_1, \eta_2, \dots, \eta_N | s_{i_0})$ . Decomposing the overall distribution into the effects emanating from different

<sup>11</sup> One possible approach consists in assuming the variables to be independent, factorize the function  $\Phi$  and compute it as in the first round. Another possibility is to use a mean field approximation to derive approximate solutions to the first moments of the distribution.

<sup>12</sup> In the Appendix we show how to compute those variables.

<sup>13</sup> It is easy to see that :

$$P_i^l = (1 - P_i^I)(1 - P_i^{II}) \dots (1 - P_i^{l-1}) \cdot \left[ 1 - \prod_{j_1=1, j_1 \neq i}^N \dots \prod_{j_l=1, j_l \neq i}^N \left( 1 - p_{ij_1} P_{j_1}^{(l-1)} \dots p_{j_{l-1}j_l} P_{j_{l-1}}^{II} P_{j_l}^I \right) \right] \quad (30)$$

which is the probability for node  $i$  not to belong to shells  $1, 2, \dots, l-1$ , multiplied by the probability for at least one  $l$ -length path to exist connecting node  $i$  and node  $i_0$ .

<sup>14</sup> Numerically we saw from the simulations that a good approximation is typically obtained for  $t \cong 20$ , and after  $t \cong 7$  rounds one obtains about 95% of all defaults observed in the simulations.

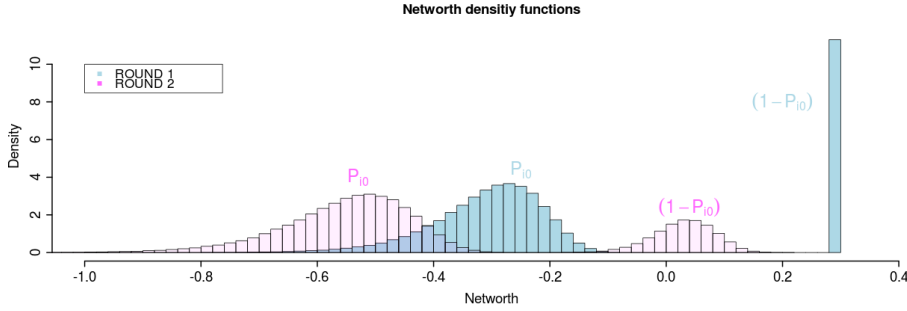


**Fig. 5:** The figure shows the temporal evolution of the marginal  $\Phi$ -function from round  $t = 1$  (cyan distribution) to round  $t = 2$  (pink distribution), for a particular bank  $i$ . At  $t = 2$ , due to the small diameter of the present network, also the contribution linked to  $(1 - p_{ii_0})$  spreads, adding a second contribution to the probability for bank  $i$  to fail.

"shells", we can write the stationary distribution as:

$$\Phi_i^\infty(\eta_i | s_{i_0}) = \sum_{l=1}^{\infty} P^l \cdot \Phi_i^{\infty, l}(\eta_i | s_{i_0}) \quad (31)$$

With a finite diameter  $d$  of the network it can be reduced to:

$$\Phi_i^\infty(\eta_i | s_{i_0}) = \sum_{l=1}^d P^l \cdot \Phi_i^{\infty, l}(\eta_i | s_{i_0}) \quad (32)$$

since  $P^l$  is equal to zero for each  $l$  equal or higher than  $d$ . Note that for any of the  $l$  components in eq. (32) a long-lasting sequence of aftereffects can result since any possible defaults would lead to the possibility of subsequent defaults in the next period of events whose losses are exceeding their (remaining) equity level and so on. So, in principle, along the time dimension, the sequence of events and, therefore, flow of probability between different states, evolves for much longer than along the dimension of shells. Typically, however, the macroeconomic statistics emerge after a relatively small number of iterations. This holds particularly for the number of defaults as these are binary counts that only change if losses exceeds threshold value, and so, higher-order knock-on effects would at some period not trigger any more defaults. We will see that the additive components of eq. (31) play a fundamental role in understanding the results from the simulation engine, and they are directly related to the network structure through the coefficients  $P^l$ .

Figure 6 shows a possible final equilibrium state for the system. In particular, the mean values of the  $d = 2$  components of the marginal  $\Phi$ -functions (32) are plotted for some banks<sup>15</sup>. We note here the differences

<sup>15</sup> Note that in the framework generated by eq. (14)  $P_i^I + P_i^{II} \simeq 1$ .

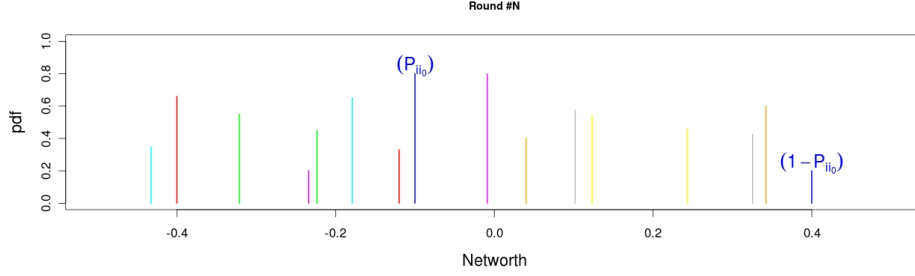


**Fig. 6:** The figure shows a possible final equilibrium state for the system; in particular, different colors represent the marginal distribution of different banks belonging to the IbM, after the shock has been absorbed. Still for each node the  $\Phi$ -function can be decomposed into two components depending on whether they have been hit immediately after the shock or at a later stage. This is illustrated by the two different entries for each bank (each color).

in information contained in the  $\Phi$ -function and in the number of defaults obtained via eq. (3): although a bank might have a positive mean value in one (or both) of the two contributions that appear in eq. (32), the probability for that bank to fail might nevertheless not be zero. This effect is not caught by eq. (3), but it is correctly quantified via the  $\Phi$ -function, that contains all the information regarding the state of the system.

In the following subsection, we explore how the main parameters affect the stability of the banking system under the failure of the largest bank.

## 5 Computational Experiments

### 5.1 The role of bank capitalization

In our first computational experiment we investigate the effects of banks' net worth on the resilience of the entire banking system. The parameter  $\theta$  will be fixed at 0.8, so that each bank will invest 20% of its total assets in the interbank market, and the remaining 80% in some external assets. We will let the parameter  $\eta$  vary from 0 to 0.1<sup>16</sup>. In all that follows, the number of banks will be fixed at  $N = 250$ . The design of the simulations will be the same for all the following experiments: the first step consists in generating one Monte Carlo realization of our banking system as explained in sec. 3. In the second step we destroy the largest bank: this shock is assumed to wipe out all the external assets from the balance sheet of the initially failing bank. For each simulation run, we count the overall number of defaults, as well as the number of defaults in each single phase of the shock propagation. We report the average number of defaults across all banks. We will use

<sup>16</sup> Remember that by mere rescaling  $\eta$  could also be interpreted as the excess over the required minimum capital requirement.

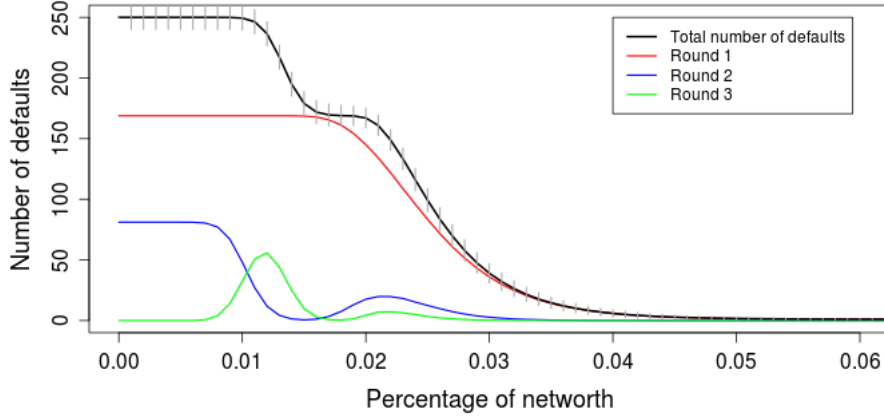


**Fig. 7:** Number of defaults as a function of the percentage of net worth  $\eta$ , for probability function 14. The other parameters are fixed at:  $\theta = 0.8$ ,  $a = 5$ ,  $b = 100$ . The picture shows both the total number of defaults (bold black line) together with the standard deviation of the mean value (small gray bars), and the number of defaults occurring during the first four phases of the propagation of the shock.

probability functions (14) with parameters  $\alpha = 0.2$ ,  $\beta = 1.2$ . Furthermore the two limits  $a$  and  $b$  will be fixed at 5 and 100 respectively<sup>17</sup>. Fig. 7 shows the result of the pertinent Monte Carlo simulations: we report both the total number of defaults (black bold line), and the number of defaults in the first four phases of the propagation of the shock. The thin vertical bars represent the standard deviation of the black line across our 200 replications of the simulations.

As one could expect, when the percentage of net worth tends to zero, the total number of defaults increases to 250: in particular, a threshold value ( $\eta = 0.0143$  in the figure) exists below which the system fails completely, and below  $\eta = 0.008$  it breaks down within only two rounds. This is a demonstration of the so called *small-world* effect: the diameter of this particular network is roughly about two for the largest bank belonging to the system, and so in only two rounds the shock will have reached almost any bank of the IbM. At the other end, when the percentage of net worth is beyond an upper threshold value, no defaults are reported and no domino effects set in.

Interestingly, the shape of the line describing the total number of defaults is far from linear. Starting from the value  $\eta = 0.1$ , we can observe that below the value  $\eta \cong 0.05$  the first defaults appear, and inspection shows that these typically happen for small banks connected to the initially failed bank. As  $\eta$

<sup>17</sup> Montagna and Lux (2013) investigate how these limits affect the resilience of the system.

decreases further, we observe a sharp increase in the number of defaults, and this growth stops at the value  $\eta \cong 0.02$  where the curve enters a *plateau*. Inspection of the defaults per round of propagation shows the reason for this non-linearity: at the level of net worth of the plateau, all the banks belonging to the first *shell* around the initially failed bank have failed, and the banks which are not directly connected to the first failing unit have enough net worth to survive the subsequent aftereffects of the shock. When the net worth decreases further, also the banks outside the first shell are no more able to absorb the perturbation, and the total number of defaults sharply moves up to 250.

It is interesting to look in more detail at the number of defaults in the different rounds. In the first round (red line in Figure 7), banks that fail are directly connected to the initially shocked bank, and when the red line reaches its *saturation* at  $\eta \cong 0.018$  the complete first *shell* (composed on average of 153 units) has failed. We note that the saturation point of the number of defaults in the first round does not coincide exactly with the *plateau* of the total number of defaults: the explanation is that with slightly higher equity levels the largest banks in the first shell need more than one hit to fail, and so they populate the failures of higher rounds. The reason for this is that for larger banks the overall number of credit relationships to other banks (by assumption, following observed empirical regularities) is higher on average and so for them the failure of the largest bank will lead to a proportionally smaller loss than for the smaller client banks of the defaulted entity. When the percentage of net worth decreases, these defaults occur already in earlier rounds, up to a point in which all banks of the first shell are affected in the first round of defaults.

The theoretical counterpart of the shapes appearing in Fig. 7 can be provided by the analytical framework of Sec. 4. In particular, we can compute the number of expected defaults due to first round effects by inserting eq. (1) in (3). In the top left panel of the figure, a comparison between the simulation results and the results obtained via eqs. (27) and (28) for the effects in the first round is shown. In the second and third panels (upper right-hand side and lower left-hand side) we represent the contributions, respectively, from the first shell during the second round, and from the second shell during the second round. The results are now obtained via a numerical algorithm (see Appendix for more details), which provides the advantage that these two contributing factors can be clearly distinguished from each other. In particular, the hump in the number of defaults in the second round is caused by banks from the first shell that have survived the first round of knock-on effects but are too fragile to survive the second wave of losses in round 2. In a similar way it is possible also to compute all effects in the other rounds.



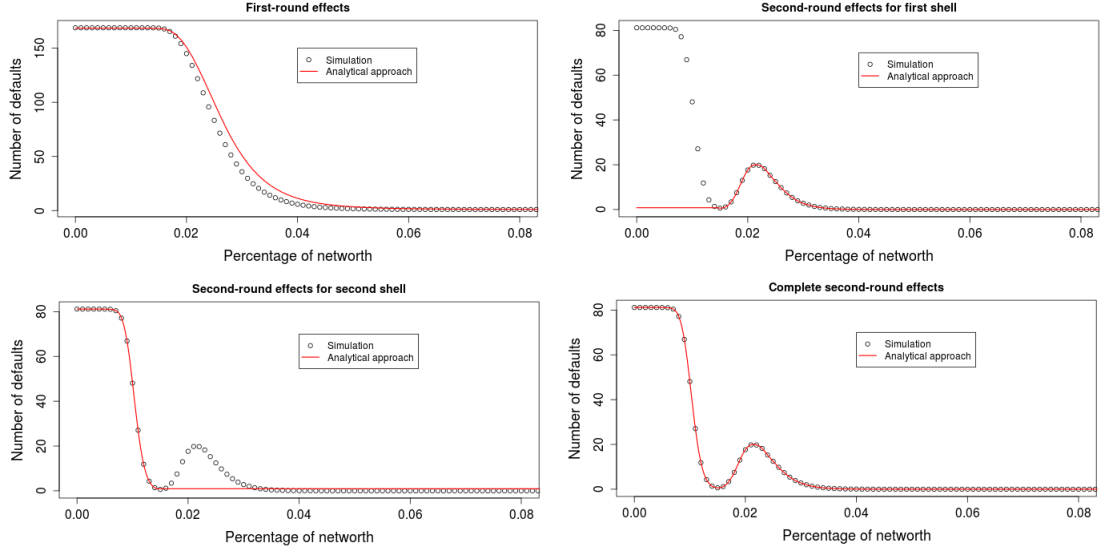


**Fig. 8:** In the four panels we show the expected number of defaults as a function of the percentage of net worth  $\gamma$ , for the first two rounds. In particular, the first panel (top-left) contains a comparison between the simulation result and the probabilistic approach varying the percentage of net worth; the red line is computed combining eqs. (28) and (3). The slight difference in the two lines is due to the application of the Central Limit Theorem in the computation of eq. (28) (see Appendix), and it will tend to zero as the number of nodes increases. The second and third panels (top-right and bottom-left) highlight the role of different shells in the spread of the shock. In particular, the two contributions linked to eq. (29) are compared with the simulation results. The last panel (bottom-right) shows a comparison between the simulation results and the analytical approach for the second round.

## 5.2 Interbank exposure

In this section we are going to explore how the number of defaults is affected by the percentage of interbank exposure as a function of total assets, namely how the parameter  $\theta$  affects the resilience of the system. An increase in interbank assets produces, as an immediate result, an increase in the weight of each edge, and so an increase of the channels through which the shock can propagate. This effect can potentially increase the number of defaults in the system, as the amount of losses transmitted to creditor banks will increase as well. On the other hand, an increase in interbank exposure implies a reduced relative exposure to external markets, and since here we are considering, as initial source of the shock, a loss in value of external assets, this second effect could reduce the systemic risks from defaults of single banks.

The design of the simulations will remain the same as in the first experiment: we generate a realization of the system and we shock the biggest bank, wiping out all its external assets. Subsequently we count the number of defaults. We will show the mean value of those numbers for each round,

and the standard deviation for the total number of defaults. In this section, the percentage of net worth  $\eta$  is fixed at 0.025, while the percentage of external assets on total assets,  $\theta$ , varies from 0.5 to 1 (when  $\theta$  is equal to one no interbank assets are present in the bank balance sheets). Fig. 9 shows the result.

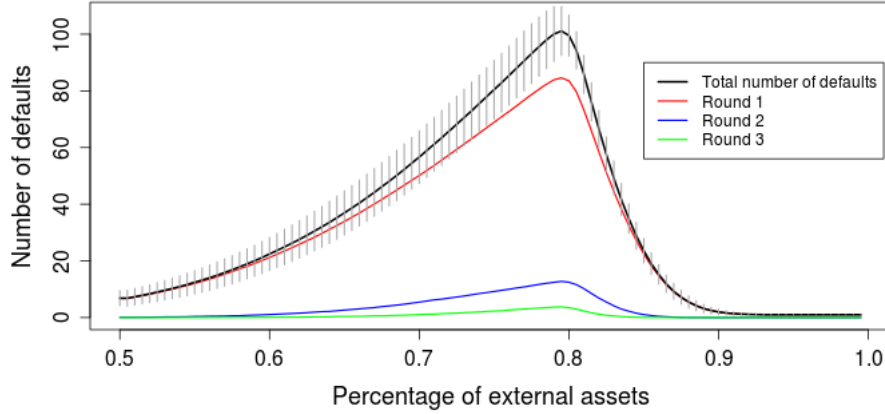


**Fig. 9:** Number of defaults as a function of the percentage of external assets  $\theta$ , i.e. 1— the percentage of interbank exposure  $\theta$ , for probability function (14). The other parameters are fixed at:  $\eta = 0.025$ ,  $a = 5$ ,  $b = 100$ . The picture shows both the total number of defaults (bold black line) together with the standard deviation of the mean value (small gray bars), and the number of defaults occurring during the first four phases of the propagation of the shock.

Overall results are similar to those reported for similar experiments in Nier *et al.* (2008). First, we note that when  $\theta$  tends to 1 the number of defaults tends to zero: in this case the banks' balance sheets contain only external assets, and so the channels for the propagation of the shock become smaller and smaller, until  $\theta$  assumes the value 1 and there are no more links in the network, and no domino effects are possible. We can also note a threshold value at  $\theta \cong 0.78$ : at this value, the contagion effects reach their maximum while both more or less intense interbank linkages reduce the number of knock-on defaults (due to a higher degree of risk sharing on the left and fewer links for contagion on the right). At the other extreme, when  $\theta$  tends to 0, banks become completely isolated from any external market, and so in our model, where the initial source of the shock comes from the external assets of the largest bank of the system, the number of defaults tends to zero as well. Note that this exercise does not leave the size of the internal shock unaffected. Clearly, when external assets decline in their absolute size (from right to left) there should be a decrease of contagious defaults.

A comparison with the analytical solution is shown in Fig. 10. The trend

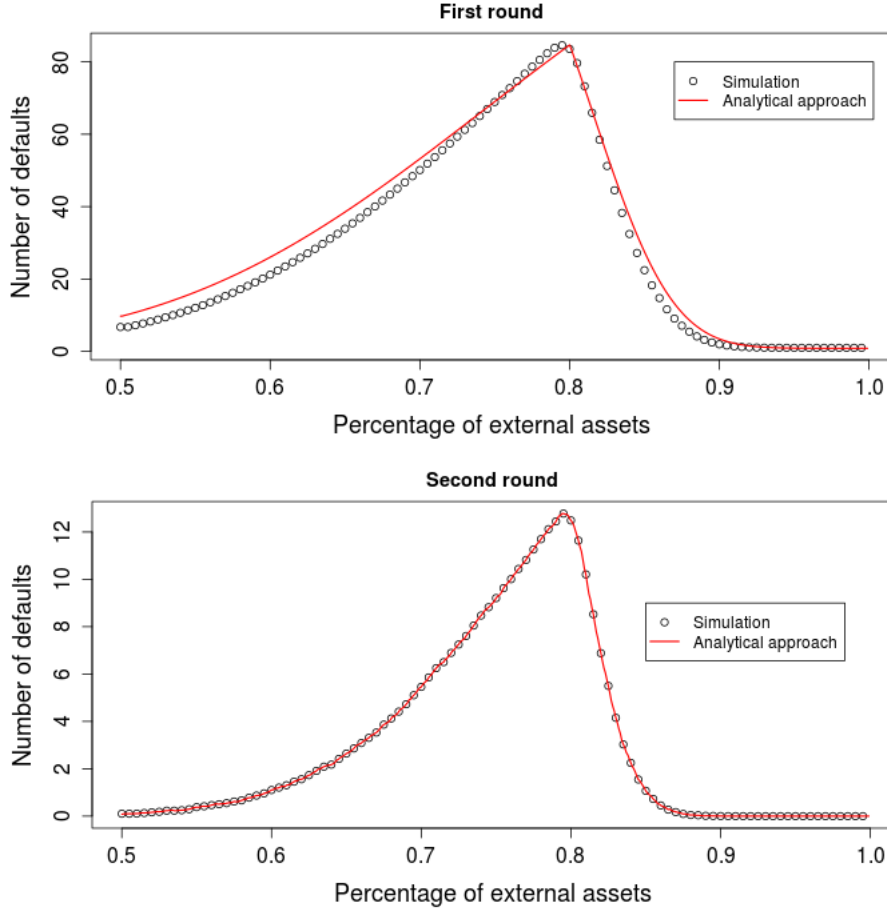


**Fig. 10:** Simulations and analytical results for the number of defaults with varying percentage of external assets.

in the number of defaults can be easily understood by studying the properties of the  $\Phi$ -function (28). In fact, as we show in the Appendix, the parameter  $b_i$  appearing in the distribution of  $\eta_i$  include the expected losses coming from the loan to the initial failing bank. These losses monotonically decrease as the percentage of external assets over total asset increases, since the initial failing bank is less exposed to idiosyncratic external shock. Interestingly, here the second-round effects exhibit basically the same pattern as those observed in the first-round of knock-on effects.

## 6 Correlated Shocks and Systemic Risk

In the computation of the  $\Phi$ -functions we have so far assumed that the initial shock to the system was a percentage of the external assets wiped out from the balance sheets of a bank in the network. In reality the banks'

balance sheets shocks are also random events, and in order to assess the financial stability of a banking system one should combine the information regarding banks profit/loss distribution with structural information on the interbank network. In our probabilistic framework, this can be captured by assigning a distribution for the initial shocks to the external parts of banks balance sheets. Here we present a simple example for correlated shocks, and we later discuss the importance of interbank credit on the propagation of idiosyncratic risk in the network.

As a suitable candidate for the loss distribution of the loan portfolio we adopt the formulation of Vasicek (1987)<sup>18</sup>:

$$v(\Lambda_i; p, \tau) = \sqrt{\frac{1-\tau}{\tau}} \exp \left( -\frac{1}{2\tau} (\sqrt{1-\tau} G^{-1}(\Lambda_i) - G^{-1}(p))^2 + \frac{1}{2} (G^{-1}(\Lambda_i))^2 \right) \quad (33)$$

where  $0 \leq \Lambda_i \leq 1$  is the percentage losses of the loan portfolio, according to the notation introduced in Sec. 2,  $p$  and  $\tau$  are parameters of the distribution, and we indicate with  $G(\cdot)$  the Normal standardized cumulative distribution function. As shown by Vasicek, eq. (33) characterizes the loss distribution of a large portfolio under the assumption of individual loan values following a logarithmic Wiener process. In this setting, banks' shocks are drawn from the probability distribution function (33), but for the time being we assume no lending relationships exist among the institutions. Hence, according to the notation introduced in Sec. 3, we set  $\theta = 1$ . Moreover, we introduce a correlation  $\rho$  among the shock variables  $\Lambda_i$ :

$$\text{cor}(\Lambda_i, \Lambda_j) = \delta_{ij} + (1 - \delta_{ij})\rho \quad (34)$$

The correlation, of course, leaves the marginal distributions for the single shocks unchanged. We set the net worth of each bank equal to the  $\alpha$ -quantile of the distribution (33), meaning that the probability of default of each single institution is  $\alpha$ , and we use in the example below  $\alpha = 0.05$ . Our first goal is to show that, also if there is no contagion process, the probabilistic framework introduced in Sec. 2 can still be usefully applied to understand and quantify the financial stability of the system. In fact, for a given level of correlation  $\rho$ , we can study the  $\Phi$ -function of the system when a vector of stochastic shocks hits the system. The shock  $S$  takes here the form of a vector of random variables  $\vec{\Lambda}$ , where each component has a distribution described by eq. (33), and the correlation among the variables is defined by eq. (34). We want to study the function  $\Phi(\vec{\eta}|\vec{\Lambda})$  to analyze the systemic risk in the system.

We compute again the expected value of the number of defaults after a shock hits the system and the  $q$ -quantile of the distribution of the number of

---

<sup>18</sup> In all what follow we use the parameters  $p$  and  $\tau$  equal respectively to 0.1 and 0.2 in eq. (33).

defaults, as defined in eqs. (3) and (7). When the correlation among banks' balance sheets is increasing, keeping the marginals constants, the expected number of defaults computed as in eq. (3) remains constant. Nevertheless, as the correlation increases the probability to have tail events (i.e. the probability to have large number of defaults) increases as well.

Figure 11 shows different measures representing the stability of the system as a function of the correlation among banks' balance sheets, for the example discussed above. In particular, the average number of defaults (computed according to eq. (3)), the 5th quantile of the distribution  $\phi(\tilde{N}|\tilde{\Lambda})$  (computed according to eq. (7)), and the maximum and the median of the same distribution are plotted. As one can see from the figure, the expected number of defaults remains unchanged (the mean is not affected by the correlation). Nevertheless, the risk for tail events increases dramatically with the correlation. In the right side of the figure, we plot the distribution of the number of defaults for the two cases  $\rho = 0$  and  $\rho = 0.5$ , to show how the overall distribution of outcomes changes.

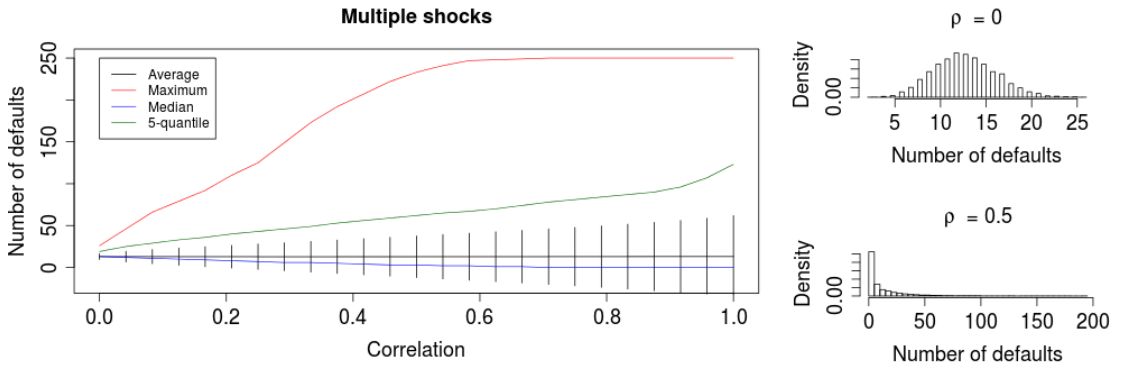


**Fig. 11:** Systemic risk measures in a banking system without interbank credit. On the left, some systemic risk statistics are plotted as functions of the correlation between banks' balance sheets. In particular, the mean number of defaults (eq. (3)) is seen to be constant, while the extreme 5th-quantile of the distribution of the number of defaults (eq. (7)) and the maximum number of defaults are seen to increase. On the right, the distribution of the number of defaults is shown for two values of the correlation  $\rho$ .

We now expand the example above by allowing again for interbank loans. The shock  $S$  assumes the same stochastic form  $\tilde{\Lambda}$  described in the previous section, and again we are interested in varying the correlation  $\rho$  among the shocks experienced by individual banks. The parameter  $\theta$ , i.e. the fraction of external assets over total assets, will now be fixed at 0.8. The equity of the banks will be determined as the regulatory minimum: it consists of the sum of the lower 5th quantile of the distribution of portfolio losses expressed in eq. (33) and a fraction  $\gamma$  of their interbank assets, we use  $\gamma = 0.02$ . This

scenario roughly reflects the standard Basel requirements, where investments are weighted according to their risk, and interbank loans have a fixed risk weight independently of the counterparty's identity.

The results are shown in the same fashion as in the previous case. While, again, the mean value  $\langle \tilde{N} | S \rangle$  remains constant, the probability for systemic events increases. A numerical comparison illustrates the differences: for a value of the correlation  $\rho$  equal to 0.2, the maximum number of defaults is 108 for the case without interbank connections, and 195 for the case where interbank loans are present. Equivalently, the last 5<sup>th</sup> quantile moves from 39 in the first case to 51 in the second case. Despite the apparently moderate level of correlation of portfolio risk, the probability of systemic events is drastically increasing in the presence of interbank connections.

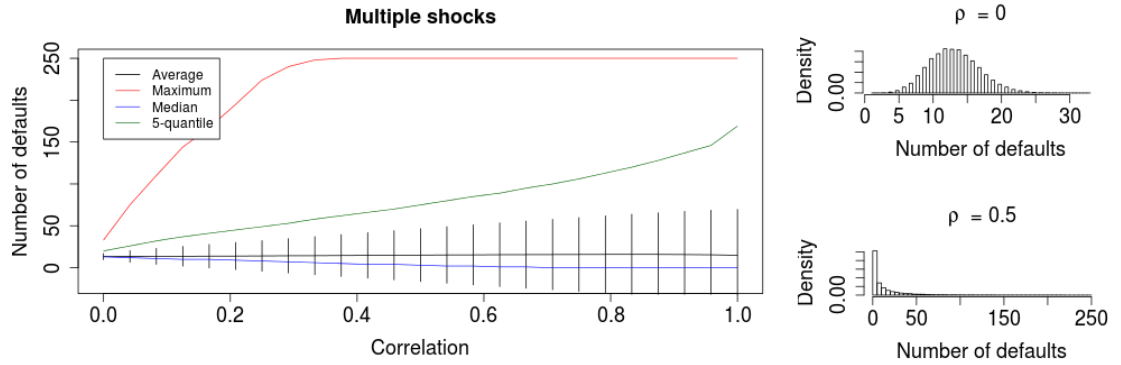


**Fig. 12:** Systemic risk measures in a banking system where interbank loans are present. On the left, some systemic risk statistics are plotted as functions of the correlation between banks' balance sheets. In particular, the mean number of defaults (eq. (3)) is seen to be constant, while the extreme 5<sup>th</sup>-quantile of the distribution of the number of defaults (eq. (7)) and the maximum number of defaults are seen to increase. On the right, the distribution of the number of defaults is shown for two values of the correlation  $\rho$ .

## 7 Conclusion

We have introduced an analytical formulation for the assessment of systemic risk through interbank contagion, and we tested our framework on a simulated financial system. The latter is generated with an algorithm that reproduces the main important topological features of a real banking system, which are the disassortative link formation and the power law behavior of the degree distribution. Moreover, heterogeneity in bank sizes is also taken into account, playing an important role for the stability of the banking system. The results are networks composed of a large pool of small and medium-sized banks with a dominating pattern of disassortative link

formation forming credit connections between dissimilar partners.

In this framework, we have investigated how the percentage of net worth and the percentage of interbank assets (on total assets) affects the spread of an idiosyncratic shock. The analytical apparatus allows to decompose the overall number of expected contagion effects both in terms of the sequence of events and the banks' location within the network: banks belonging to the first shell (i.e. creditor banks of the defaulted entity) fail mostly before the others, and it is possible to distinguish between defaults of the different shells in the cascade of events.

The analytical formulation of the problem is based on the concept of  $\Phi$ -functions. The  $\Phi$ -function describes, in a discrete event framework, the evolution of the state of the system. The computation of an explicit closed form for  $\Phi$  is possible only for the first round effects. Nevertheless, approximations or numerical methods can be used for higher rounds. These results, moreover, can be easily generalized to other forms of interbank contracts.

When allowing for correlation among banks' investments the probability of systemic events increases sharply even if each single unit perfectly follows the micro prudential regulation. The tails of systemic events are furthermore made fatter by direct contracts among the financial institutions, like in our example of interbank loans. In times where portfolio correlation increases, the correct assessment of the propagation of small probability events becomes crucial to assess systemic risk.

We note that the computation of the state function would not get much more complicated when using different values of  $\theta$  and  $\eta$  for each bank, and so it can be in principle used in order to assess the systemic impact of each bank on the entire system. For example, using eq. (7), it is possible to determine the risk that a regulator is willing to run in case of the default of a particular entity, for different parameters  $\theta$  and  $\eta$  (or, eventually, heterogeneous vectors  $\vec{\theta} = (\theta_1, \theta_2, \dots, \theta_N)$  and  $\vec{\eta} = (\eta_1, \eta_2, \dots, \eta_N)$  if, for example, different capital requirements depending on different systemic impact level were imposed). In terms of the systemic impact of a default, eq. (3) provides the expected number of triggered defaults in case of insolvency of a particular entity: the implementation of this expression using empirical data can help in quantitatively identify institutions that are too-big-to-fail and too-interconnected-to-fail. Overall, the framework of Sec. 3 is sufficiently flexible and general to accommodate whatever knowledge is available on the structural details of the interbank market. With complete knowledge of all links and exposures, the exact extent of knock-on effects could be determined as well as the identity of defaulting units. If we only know some boundary conditions (like the distribution of balance sheet sizes) and have an informed guess on others (link distribution and distribution of mutual exposures in our present application), expected knock-on effects, quantiles, value-at-risk and other interesting quantities can be computed numerically. We note

here that the lack of analytical results for higher rounds is not a major obstacle as the closed-form solutions can easily be replaced by their numerical counterparts.

## References

- [1] Acemoglu, D., Ozdaglar, A., Tahbaz-Salehi, A., "Systemic Risk and Stability in Financial Networks", NBER Working Paper No. 18727 (2013)
- [2] Adrian, T., Brunnermeier, M. K., "CoVar", NBER Working Paper No. 17454, (2011)
- [3] Allen, F. and Gale, D., "Financial contagion", *Journal of Political Economy*, Vol. 108, pages 1-33, (2000)
- [4] Battiston, S., Delli Gatti, D., Gallegati, M., Greenwald, B. & Stiglitz, J. E., "Liaisons dangereuses: increasing connectivity, risk sharing, and systemic risk", *Journal of Economic Dynamics and Control*, Volume 36, Issue 8 (2012a)
- [5] Battiston, S., Puliga, M., Kaushik, R., Tasca, P., and Caldarelli, G., "DebtRank: Too Central to Fail? Financial Networks, the FED and Systemic Risk", *Scientific Report*, doi:10.1038/srep00541, (2012b)
- [6] Benito, E., "Size, growth and bank dynamics", *Documento de Trabajo*, Banco De España, (2008)
- [7] Bluhm, M., Faia, E., Krahnen, J. P., "Endogenous Banks' Networks, Cascades and Systemic Risk", SAFE Working Paper No. 12, (2013)
- [8] Boss, M., H. Elsinger, M. Summer, and S. Thurner, "Network topology of the interbank market", *Quantitative Finance*, 4(6), 677-684, (2004)
- [9] Brunnermeier, Markus K., "Deciphering the Liquidity and Credit Crunch 2007-2008", *Journal of Economic Perspectives*, Volume 23, Number 1, p.77-100, (2009)
- [10] Caldarelli, G., "Scale-Free Networks: Complex Webs in Nature and Technology", Oxford University Press, (2007)
- [11] Censor, Y. and Zenios, S.A., "Parallel optimization", *Oxford University Press*, (1997)



- [12] Cocco, J. F., Gomes, F. J., Martins N. C., "Lending relationships in the interbank market", *Journal of Financial Intermediation* 18, pp. 24-48, (2009)
- [13] De Masi, G., Iori, G., and Caldarelli, G., "Fitness model for the Italian interbank money market", *Physical Review E* 74 066112, (2006)
- [14] Glasserman P., Young P. H., "How likely is contagion in financial networks?", *Journal of Banking & Finance*, in press, (2014)
- [15] Ennis, H. M., "On the size distribution of banks", *Federal Reserve Bank of Richmond Economic Quarterly*, 87, pp. 1-25, (2001)
- [16] Finger, K., Fricke, D., Lux, T., "Network Analysis of the e-MID Overnight Money Market: The Informational Value of Different Aggregation Levels for Intrinsic Dynamic Processes", *Computational Management Science*, Volume 10, Issue 2-3, pp 187-211 (2013)
- [17] Gai, P. and Kapadia, S., "Contagion in Financial Networks", *Proceedings of the Royal Society A*, 466, 2401-2403, (2010)
- [18] Gai, P., Haladane, A., Kapadia, S., "Complexity, concentration and contagion", *Journal of Monetary Economics*, Volume 58, Issue 5, Pages 453–470 (2011)
- [19] Georg, C., "The effect of interbank network structure on contagion and common shocks", *Journal of Banking & Finance* 37(7), Pages 2216–2228 (2013)
- [20] Haldane, A. and May, R., "Financial Systems: Ecology and Economics", *Nature* 469, (2011)
- [21] Imakubo, K., Soejima, Y., "The Transaction Network in Japan's Interbank Money Market", Financial market department, Bank of Japan, *Financial System Report*, (2006)
- [22] Inaoka, H., T. Ninomiya, K. Taniguchi, T. Shimizu, and H. Takayasu, "Fractal Network Derived from Banking Transaction: An Analysis of Network Structures Formed by Financial Institutions", Bank of Japan Working Paper No. 04-E-4, Bank of Japan, (2004)

- [23] Iori, G., de Masi, G., Precup, O., Gabbi, G., and Caldarelli, G., "A Network Analysis of the Italian Overnight Money Market", *Journal of Economics and Dynamics & Control*, 32, pp. 259–278, (2008)
- [24] Janicki, H. P., and Prescott, E. C., "Changes in the size distribution of U.S. banks: 1960-2005", *Federal Reserve Bank of Richmond Economic Quarterly*, 92, pp. 291-316, (2006)
- [25] Luttmer, E. G. J., "Selection, Growth, and the Size Distribution of Firms", *The Quarterly Journal of Economics*, 122 (3): 1103-1144 (2007)
- [26] Lux, T., Fricke, D. "Core-Periphery Structure in the Overnight Money Market: Evidence from the e-MID Trading Platform", *Computational Economics*, <http://dx.doi.org/10.1007/s10614-014-9427-x>, in press, (2014)
- [27] May R., and Arinaminpathy, N., "Systemic risk: the dynamics of model banking systems", *Journal of the Royal Society Interface* 6, vol. 7 no. 46, 823-838, (2010)
- [28] Memmel, C., Sachs, A., "Contagion in the interbank market and its determinants", Deutsche Bundesbank, *Discussion Paper*, Series 2: Banking and Financial Studies. No 17/2011, (2011)
- [29] Mistrulli, P. E., "Assessing financial contagion in the interbank market: Maximum entropy versus observed interbank lending patterns", *Temi di discussione*, N 641 (working papers), (2007)
- [30] Montagna, M., and Lux, T., "Hubs and resilience: towards more realistic models of the interbank markets", *Kiel Working Paper*, 1826, Kiel Institute for the World Economy, Kiel, (2013)
- [31] Nier, E., Yang, J., Yorulmazer, T., and Alentorn, A., "Network models and financial stability", *Journal of Economic Dynamics & Control* 31, (2007)
- [32] Newman, M., "Random Graphs as Models of Networks", in Bornholdt, S. and H. Schuster, eds., *Handbook of Graphs and Networks: From the Genome to the Internet*, Wiley (2003)
- [33] Soramäki, K., Bech, M. L., Arnold, J., Glass, R. J., and Beyeler, W., "The topology of Interbank Payment Flows", *Staff Report*, 243, Federal Reserve Bank of New York, (2006)
- [34] Upper, C., "Simulation methods to assess the danger of contagion in interbank markets", *Journal of Financial Stability*, doi:10.1016/j.jfs.2010.12.001, (2011)

- [35] Upper C. and Worms A., "Estimating Bilateral Exposures in the German Interbank Market: Is there a Danger of Contagion?", *European Economic Review*, 8, 827-49, (2004)
- [36] Vasicek, O., "Probability of Loss on Loan Portfolio", KMV Corporation (available at *kmv.com*), (1987)

## A Computation of the state functions: analytical solutions for first round effects

The purpose of this appendix is to provide the derivation of eqs. (28) and (29). We first recall the main characteristics of the model; a probability matrix  $P$ , with entries  $p_{ij} = P_s(A_i, A_j)$  ( $s = 1, 2, 3$ ), indicates the probability for each possible edge in the system, this is computed after the sequence  $\{A_i\}$  has been assigned to the system itself. For each probability matrix  $P$ , a large number of realizations for the adjacency matrices are possible. Once an adjacency matrix  $A$  has been determined for the system, the weight of each edge is computed according to:

$$l_{ij} = \frac{l_i p_{ij}}{\sum_{j \in \Omega_i} p_{ij}} = \frac{(1 - \theta) A_i p_{ij}}{\sum_{j \in \Omega_i} p_{ij}} \quad (35)$$

where  $\Omega_i$  denotes the set of nodes which satisfy  $a_{ij} = 1$ . We can now start deriving eq. (28). First of all, note that with probability  $(1 - p_{ij})$ , bank  $i$  has no link directed to bank  $i_0$ , and in that case its net worth  $\eta_i$  in round 1 rests unchanged and remains identical to  $\eta_i^0$ : this situation gives one of the two contributions in eq. (28). In the other case ( $a_{ij} = 1$ ), we have instead:

$$\eta_i^{r=1} = \eta_i^1 = \eta_i^0 - f_{i_0} l_{ii_0} = \eta_i^0 - f_{i_0} \frac{(1 - \theta) A_i p_{ii_0}}{c_i} \quad (36)$$

where  $\eta_i^1$  is the net worth of bank  $i$  at time  $t = 1$ ,  $f_{i_0}$  is the fraction of money that bank  $i_0$ 's creditors lose due the failure of bank  $i_0$ , and  $c_i = \sum_{j \in \Omega_i} p_{ij}$ . Considering the mechanism of contagion explained in section 4, we have:

$$f_{i_0} = f_{i_0}(\theta, \gamma) = \min \left[ \frac{(1 - \theta) A_{i_0} - \gamma A_{i_0}}{\sum_j p_{ji_0}}, 1 \right] \quad (37)$$

To derive the distribution of the random variables  $\eta_i$  we note that on the right side of eq. (36) the only random term is  $c_i$ , since the other are fixed once the sequence  $\{A_i\}$  and the probability matrix  $P$  are fixed. We can write:

$$c_i = \sum_{j=1}^n \theta (P_s(A_i, A_j) - \xi_j) \cdot P_s(A_i, A_j) = \sum_{j=1}^n c_{ij} \quad (38)$$

where  $\theta(x)$  denotes again the Heaviside function and  $\xi_i$  are *i.i.d.* random variables with uniform distribution between zero and one:

$$\xi_i \sim U_{[0,1]} \quad (39)$$

Since we are using  $N = 250$ , and the variables in eq. (38) are simply functions of *i.i.d.* random variables with finite mean and variance, we can apply the Central Limit Theorem (CTL) and conclude that  $c_i$  can be approximated by a Gaussian distribution with mean:

$$\begin{aligned} \langle c_i \rangle &= \sum_{j=1}^n \langle \theta(P_s(A_i, A_j) - \xi_j) \cdot p_{ij} \rangle \\ &= \sum_{j=1}^n \int_0^1 \rho(\xi) \theta(P_s(A_i, A_j) - \xi_j) \cdot p_{ij} d\xi \\ &= \sum_{j=1}^n p_{ij} \int_0^{p_{ij}} d\xi = \sum_{j=1}^n p_{ij}^2 \equiv m_i, \end{aligned} \quad (40)$$

and variance:

$$\begin{aligned} \sigma_{ij}^2 &= \text{Var}[\theta(P_s(A_i, A_j) - \xi_j)] = \langle c_{ij}^2 \rangle - \langle c_{ij} \rangle^2 \\ &= \left( \int_0^1 d\xi [\theta(P_{ij} - \xi_j)]^2 p_{ij}^2 \right) - p_{ij}^4 = p_{ij}^3 - p_{ij}^4, \end{aligned} \quad (41)$$

and so:

$$\sigma_i^2 = \sum_{j=1}^n \sigma_{ij}^2 = \sum_{j=1}^n (p_{ij}^3 - p_{ij}^4). \quad (42)$$

Therefore, the distribution of the variables  $c_i$  can be approximated by:

$$\rho(c_i) = \frac{1}{\sigma_i \sqrt{2\pi}} \cdot \exp \left\{ -\frac{1}{2} \left( \frac{c_i - m_i}{\sigma_i} \right)^2 \right\}. \quad (43)$$

Now we have to compute the distribution of  $\eta_i^1$ , which is a simple function of  $c_i$ . Rewriting eq. (36) as:

$$\eta_i^1 = \eta_i^0 - f_{i0} \frac{(1 - \theta) A_i p_{ii0}}{c_i} = a - \frac{b}{c_i} \quad (44)$$

where we indicate the constant terms  $\eta_i^0$  and  $f_{i0} (1 - \theta) A_i p_{ii0}$  with  $a$  and  $b$  respectively. Denoting by  $\rho_c(\cdot)$  the pdf of  $c_i$ , we obtain the pdf of  $\eta_i^1$  as follows:

$$\begin{aligned}
\rho(\eta_i^1) &= \frac{\rho_c\left(\frac{b}{a-\eta_i^1}\right)}{\left|f'\left(\frac{b}{a-\eta_i^1}\right)\right|} = \frac{b}{(a-\eta_i^1)^2} \cdot \rho_c\left(\frac{b}{a-\eta_i^1}\right) \\
&= \frac{b}{(a-\eta_i^1)^2} \cdot \frac{1}{\sigma_i \sqrt{2\pi}} \cdot \exp\left\{-\frac{1}{2} \left(\frac{\frac{b}{a-\eta_i^1} - m_i}{\sigma_i}\right)^2\right\}
\end{aligned} \tag{45}$$

where  $a$  and  $b$  depend on  $\eta$  and  $\theta$ . The last equation, combined with the Dirac delta for the variable  $\eta_i$ , leads us to eq. (28). Note that in the case of a random network, the individual determinants  $m_i$  and  $\sigma_i$  would be constant across banks while they depend on the balance sheet size through eq. (14) to (16) in the present framework.

As regards the state function of the second round,  $\Phi^{t=2}(\vec{\eta}|s_{i_0})$ , since the variable  $\eta_i$ s are now dependent, an explicit closed form becomes difficult to compute (and the same is true for all the other higher rounds). However, it is possible to use different approximations of these state functions. One way is the factorization of the function itself as:

$$\Phi^{t=2}(\eta_1, \eta_2, \dots, \eta_n; s_{i_0}) = \prod_{i=0}^n \Phi_i^{t=2}(\eta_i) \tag{46}$$

assuming absence of dependency between variables. However, such an approximation leaves out some of the interesting spillover effects that are the focus of our interest. We prefer, therefore, to generate variables  $\eta_i$  and compute the integral in eq. 3 numerically. In order to generate the variables, we use the following algorithm, which is built-in into the structure of our model:

- given a probability matrix  $P$  and a sequence  $\{A_i\}$  for the node's fitness parameters, we generate a  $N \times N$  random matrix  $M$ , with entries  $m_{ij}$  distributed according to:

$$m_{ij} \sim i.i.d. , U_{[0,1]}$$

an adjacency matrix  $A$  with entries:

$$a_{ij} = \begin{cases} 1, & \text{if } m_{ij} \leq p_{ij} \\ 0, & \text{otherwise} \end{cases} \tag{47}$$

and the correspondent weight matrix  $W$  with entries  $w_{ij} = l_{ij}$ ;

- for each node we generate its second round net worth  $\eta_{i,2}$ ; with probability  $P^I = p_{ii_0}$  it will be:

$$\eta_{i,2} = \eta_i^0 - f_{i_0} l_{ii_0} - \sum_{j=1}^n \theta(p_{ij} - m_{ij}) \theta(p_{ji_0} - m_{ji_0}) \theta(P_1(a_j) - \varepsilon_j) l_{ij} f_j \tag{48}$$

with probability  $P^{II}$ :

$$\eta_{i,2} = \eta_i^0 - \sum_{j=1}^n \theta(p_{ij} - m_{ij})\theta(p_{ji_0} - m_{ji_0})\theta(P_1(a_j) - \varepsilon_j)l_{ij}f_j \quad (49)$$

and with probability  $1 - P^I - P^{II}$ :

$$\eta_{i,2} = \eta_i^0 \quad (50)$$

where  $\varepsilon_i$  are *i.i.d.* variables distributed according to a uniform pdf,  $\varepsilon_i \sim U_{[0,1]}$ , and  $P_1(a_i)$  is the probability that bank  $i$  has failed in the first round, computed according to eq. (28). In general, to generate the equity levels for higher rounds, one needs to build equations like (48) - (50) the losses coming from the banks in the lower shells of the system.

In this way the two contributions can be separated, and the output is shown in Fig. 5. The advantage of working with state functions instead of Monte Carlo realizations of the system is that we get *closer* to an analytical solution and can decompose the overall effects into their different elements.

The coefficients  $f_i$  are obtained directly from the model:

$$f_i \equiv \frac{\min[p_i \cdot e_i - \eta_i; l_i]}{l_i} = \min\left[1, \frac{A_i[p_i\theta - \gamma]}{l_i}\right] \quad (51)$$

where  $\lambda_i$  is the size of the shock, according to notation presented in Sec. 2, and we can compute a mean-field approximation to  $l_i$  as:

$$l_i = n \cdot \int_a^b \frac{1}{c_j} (1 - \theta) A_j \cdot p_{ji} \cdot \rho(A_j) dA_j \quad (52)$$

which brings us to:

$$f_i = \min\left[1, \frac{(\lambda_i\theta - \gamma)}{(1 - \theta)} \frac{A_i}{\sum_j \frac{A_j P_{ji}^2}{\sum_k P_{jk}^2}}\right] \quad (53)$$

Note that  $f_i$  represents the limited liability condition, which through the minimum functions in eq. (51) complicates the problem of finding an analytical solution for the state function at each event time  $t$  higher than 1. Since the  $c_i$ s are random variables, the expectation of  $l_i$  is obtained by substituting  $c_j$  with its expectation value, computed using eq. (43). Note that, in case the shock consists in wiping out all external assets from the balance sheets of the biggest bank  $i_0$ , it is easy to see that  $f_{i_0} = 1$  if  $\theta$  is higher than a certain threshold value: in this case no damping factor will enter in eq. (36).

## B Mean and variance for the marginal $\Phi$ -function

In this section we show how to compute the mean and variance for the state function (28). Our goal is therefore to compute mean and variance of the variable (44), given that  $c_i$  is distributed according to (43). In general, given a random variable  $x$ , distributed according to  $\rho_x(x)$ , and a variable  $y$  defined as a function of the former,  $y = f(x)$ , it is possible to find an approximation for the mean and the variance of  $y$  through the following method. As regards the mean, we have:

$$\langle y \rangle = \langle f(x) \rangle = \langle f(\mu_x + (x - \mu_x)) \rangle \quad (54)$$

where we call  $\mu_x$  the mean value of the variable  $x$ . A Taylor expansion around  $\mu_x$  leads to:

$$\langle f(\mu_x) + f'(\mu_x)(x - \mu_x) + \frac{1}{2}f''(\mu_x)(x - \mu_x)^2 + \frac{1}{3!}f'''(\mu_x)(x - \mu_x)^3 + \dots \rangle \quad (55)$$

In case of a Gaussian variable, the above equation reduces to:

$$\langle y \rangle = f(\mu_x) + \frac{1}{2}f''(\mu_x)\sigma_x^2 \quad (56)$$

In our case, we know the distribution of the function  $c_i$ , which is approximated by a Gaussian distribution, and we want to know the distribution of  $\eta_i$ , defined as:

$$\eta_i = a - \frac{b}{c_i} \quad (57)$$

We have, after some algebra:

$$\langle \eta_i \rangle = \eta_i^0 - p_{ii_0} \left[ \frac{b_i}{m_i} + \frac{b_i}{m_i^3} \sigma_i^2 \right] \quad (58)$$

and

$$\langle \eta_i^2 \rangle - \langle \eta_i \rangle^2 = p_{ii_0} b_i^2 \left[ \frac{1}{m_i^2} (1 - p_{ii_0}) + \frac{\sigma_i^2}{m_i^4} (3 - 2p_{ii_0}) - p_{ii_0} \frac{\sigma_i^4}{m_i^6} \right] \quad (59)$$

It is easy to see that the above expression approaches zero if all the elements  $p_{ij}$  tend to one or to zero: the full information regarding the network structure will restore the determinism and remove all uncertainty about the extent of contagion.

## C Computation of the degree distribution and the density via the probability function

We provide here the derivation of the equations stated in sec. 3. Starting from a particular probability function  $P_S(A_i, A_j)$ , and a distribution for the

size parameter  $\rho(A_i)$ , we can write the mean in-degree of a vertex as:

$$k_{in}(A_i) = N \int_a^b P_S(t, A_i) \rho(t) dt = N \cdot F_{in}(A_i) \quad (60)$$

and, similarly, for the out-degree we can write:

$$k_{out}(A_i) = N \int_a^b P_S(A_i, t) \rho(t) dt = N \cdot F_{out}(A_i) \quad (61)$$

where  $N$  is the number of nodes of the network. Assuming the function  $F_{in}(A_i)$  and  $F_{out}(A_i)$  to be monotonous in  $A_i$ , and for  $N$  large enough, we can invert the functions  $F_{in}$  and  $F_{out}$  in order to find the relationships between the size parameter  $A_i$  and the the out-and in-degree of the node:

$$A_i = F_{in}^{-1} \left( \frac{k_{in}}{N} \right) \quad (62)$$

$$A_i = F_{out}^{-1} \left( \frac{k_{out}}{N} \right) \quad (63)$$

The transformation of the parameter in the size-distribution  $\rho(A_i)$ , from  $A_i$  to  $k_{in/out}$ , leads us to:

$$P(k_{in}) = \rho \left[ F_{in}^{-1} \left( \frac{k_{in}}{N} \right) \right] \cdot \frac{d}{dk_{in}} F_{in}^{-1} \left( \frac{k_{in}}{N} \right) \quad (64)$$

$$P(k_{out}) = \rho \left[ F_{out}^{-1} \left( \frac{k_{out}}{N} \right) \right] \cdot \frac{d}{dk_{out}} F_{out}^{-1} \left( \frac{k_{out}}{N} \right) \quad (65)$$

The density  $D^l$  of a network generated according to probability function  $P_l$  is computed as follow:

$$D^l = \frac{2 \cdot \langle n_l \rangle}{N(N-1)} = \frac{2 \cdot \sum_{i,j=1}^N \langle H(P_{ij}^l - \epsilon_{ij}) \rangle}{N(N-1)} = \frac{2 \cdot \sum_{i,j=1}^N P_{ij}^l}{N(N-1)} \quad (66)$$

where  $\langle n_l \rangle$  is the expectation value of the number of links generated by probability function  $P_l$ ,  $\epsilon_{ij}$  are i.i.d. random variables distributed uniformly over the interval  $[0, 1]$ , and  $H(\cdot)$  is the Heaviside function.